Inorganic Chemistry Communications 128 (2021) 108590

Contents lists available at ScienceDirect

Inorganic Chemistry Communications

journal homepage: www.elsevier.com/locate/inoche

Short communication

Au@Cellulose/DFNS for synthesis of thiazolidin-2-ones from arylamines, elemental sulfur and CO_2

Xingyue Wei *, Xingmin Wang

College of Environment and Resources, Chongqing Technology and Business University, Chongqing 400067, China

ARTICLE INFO

Keywords:
Nanocatalyst
Green chemistry
Thiazolidin-2-one
Gold
Cellulose

ABSTRACT

Turning waste into valuable material is a remarkable phenomenon in sustainable chemistry. However, this reaction is not easy to perform due to the simultaneous employment of two low-reaction raw materials. In this study, we announce the employment of elemental sulfur and CO_2 in a multi-element reaction to manufacture valuable thiazolidin-2-ones in the participation of Au@Cellulose/DFNS as a catalyst. In this method, three bonds in one reaction and functional groups with good tolerance were created. To generate the catalyst, DFNS was amended with cellulose through the click reaction and employed as a support for Au nanoparticles. Cellulose acted as both decreasing and consistency medium for Au NPs and removed the need for decreasing agent. The generated catalyst was distinguished by various techniques like XPS, TEM, TGA, SEM, ICP, and XRD analyses.

1. Introduction

Due to the importance of environmental influences, huge endeavor have been made to the expansion of sustainable chemistry. The production of valuable chemicals with the help of CO_2 as a source of C1 has received much attention owing to the redundancy, accessibility, sustainability, and nontoxicity of CO_2 [1–8]. Even though the thermodynamic stability and kinetic inertia of CO_2 pose challenges for its employment in organic synthesis, different types of CO_2 alterations have been used to produce important carbonyl-containing heterocycles [9–14]. Lately, carbonylation of Hydrogen–Carbon bonds with CO_2 has appeared as an extremely encouraging and impressive technique to construct various types of carbonyl-containing heterocycles formulated on the notion of "$CO_2 = [O] + CO$" [15–17]. Still, there is a strong desire to expand other green techniques for the production of carbonyl containing heterocycles through Hydrogen–Carbon functionalization.

Thiazolidin-2-ones play a significant role in loads of pharmaceuticals, agrochemicals, and natural products [18–22]. Hence, the creation of effective guideline for the eclectic synthesis of thiazolidin-2-one derivatives is of great value. Lately, many groups have considerably contributed to this domain by creating different techniques to produce thiazolidin-2-ones with a variety of carbonyl sources. However, most of the substrates are restricted to bifunctional arenes accommodate two functional groups. As far as the researchers know, the monofunctionalized substrates, like arylamines, have not been employed to generate thiazolidin-2-ones with CO_2 and one sulfur source. Elemental sulfur (S8) - that is stable, non-toxic, easy to work with, and cost-effective, is considered industrial waste [23–25] and has been employed in S–C bond development [26–32]. The researchers hypothesized whether thiazolidin-2-one derivatives could be made deploying three accessible substrates, namely, aryl amines, S8 and CO_2.

In the last decade, Gold catalysis has promptly become popular in chemistry [33]. Gold species, both as heterogeneous or homogeneous catalyst [34,35], present excellent results in a variety of reactions [36,37]. Gold NPs have deployed as extremely effective catalyst to form of C-N, C-C, C-P, C-F, C-O, and C-S bonds beginning with alkenes and alkynes [38–40]. Through the lens of the reactivity, Au complexes containing phosphorus ligands are one of the reaction categories of Au catalysts. Recyclable support for these ligands is considered a significant method to ameliorate their application in organic reactions. Recently, the employment of gold NPs bonded to solid supports has been shown to remarkably influence on blocking the aggregation of Au [41–43].

In view of the above, a new heterogeneous catalyst with immobilization of gold nanoparticles on clicked cellulose-modified DFNS NPs was generated and its catalytic charactristics in the practical triple-element reaction to produce thiazolidin-2-ones from arylamines, S_8, and CO_2 was investigated (Scheme 1).

* Corresponding author.
E-mail address: weixingyue29@163.com (X. Wei).

https://doi.org/10.1016/j.inoche.2021.108590
Received 20 February 2021; Received in revised form 14 March 2021; Accepted 26 March 2021
Available online 29 March 2021

Scheme 1. Production of thiazolidin-2-ones.

2. Experimental

2.1. The global approach for the creation of DFNS nanoparticles

Urea (1.8 g) and CTAB (3 g) were released in distilled water and mixed for 5 h to dissolve. It was then added to a blend of TEOS (7.5 g), pentanol (3.5 mL), and cyclohexane (50 mL) and blended for 45 min at r. t. It was then refluxed for 4 h at 140 °C while stirring in an oil bath. The final product was then placed in an oven at 80 °C for 20 h. The silica was isolated by centrifugation (45 min, 4000 rpm), washed with acetone as well as distilled water, and vacuum-dried for 20 h. The synthesized DFNS was then calcined at 400 °C in the air for 6 h.

2.2. The global method for the synthesis of N_3/DFNS

3-chloropropyltriethoxysilane (5 mL) was released and the blend was refluxed for 20 h. The acquired Cl/DFNS was detached from the blen-demploying a magnet and rinsed frequently with ethanol for 8 h, then dried at 100 °C for 8 h. Then, 1.5 g of Cl/DFNS was ultrasonically dispersed in a solution of 2.5 g of NaN_3 in 60 mL of dimethylformamide and the blend was mixed at 90 °C for 15 h. The acquired precipitate was magnetically collected, washed with dimethylformamide, and dried at 90 °C for 10 h to produce N_3/DFNS.

2.3. Generation of alkyne-functionalized cellulose

Cellulose (1.5 g) was suspended in 80 mL of basic aqueous solution (1.1 wt% NaOH) at r.t. for 60 min to provide it with sufficient time to inflate enough and enhance the availability of –OH groups to chemical reagents. The agent was gradually warmed to 70 °C for 60 min and the necessary amount of propargyl bromide was quickly released. Following mixing at 70 °C for 20 h, the blend was purified and rinsed with water and ethanol. Alkyne-functionalized cellulose was acquired after drying at 60 °C, and detected by FT-IR spectroscopy.

2.4. The global method for the synthesis of Cellulose/DFNS

A blend of alkyne-functionalized cellulose (2.5 g), N_3/DFNS (1.5 g), and sodium ascorbate (2.5 g) in dimethylformamide (40 mL) was mixed at 60 °C for 20 h. When the reaction blend had cooled to r.t., the outcome was detached. Then it was washed with deionized water and dimethylformamide vacuum dried at 70 °C for 10 h.

2.5. The global method for the synthesis of Au@Cellulose/DFNS

$HAuCl_4{\cdot}3H_2O$ (10 mM, 2.67 mL) was released in a blend of Cellulose/DFNS (1.5 g) in ethanol (60 mL) and ultrasonicated for 40 min. After mixing for 20 h at ambient temperature, the product was separated, washed with methanol, and dried at 100 °C for 10 h to create Au@Cellulose/DFNS.

2.6. The global method for synthesis of thiazolidin-2-one

Aniline (1.5 mmol), S_8 (1.5 mmol), Au@Cellulose/DFNS NPs (8 mg), CH_3CN (10 mL) and *t*BuOK (4 eq.) were added to a 150 mL autoclave. The closed autoclave was sanitized twice with CO_2 gas, pressurized with CO_2 (1.5 MPa), and warmed below 70 °C for 8 h. In the next step, the reaction mixture was unheated to ambient temperature, the remaining

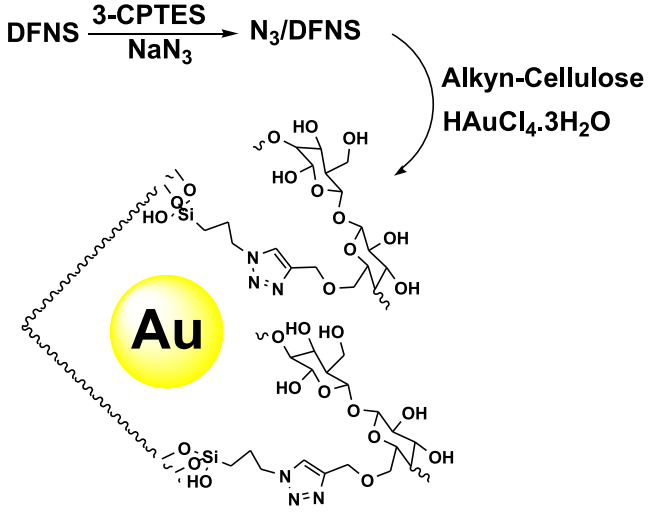

Scheme 2. Synthetic route for the preparation of Au@Cellulose/DFNS.

CO_2 gas was removed, and the reactor was opened. The reaction was controlled by TLC. After completion, ethanol was added to the reaction mixture and it was filtered to separate the catalyst. Next, the solvent was removed from the solution under dropped pressure and the outcome was cleansed by recrystallization deploying ethyl acetate/n-hexane.

2.7. Characterization data

2.7.1. Naphtho[2,1-d]thiazol-2(3H)-one

^{1}H NMR (DMSO, 400 MHz) δ 12.14 (s, 1H), 7.91 (d, J = 8.2 Hz, 1H), 7.88 (d, J = 8.6 Hz, 1H), 7.65 (d, J = 8.3 Hz, 1H), 7.59 (t, J = 8.1 Hz, 1H), 7.43 (t, J = 8.1 Hz, 1H), 7.38 (d, J = 8.7 Hz, 1H) ppm. ^{13}C NMR (DMSO, 400 MHz) δ 170.50, 133.91, 129.62, 129.54, 128.00, 127.74, 127.45, 125.07, 122.99, 117.46, 112.82 ppm.

2.7.2. 7-methylnaphtho[2,1-d]thiazol-2(3H)-one

^{1}H NMR (DMSO, 400 MHz) δ 12.02 (s, 1H), 7.76 – 7.61 (m, 2H), 7.49 (d, J = 8.4 Hz, 1H), 7.32 (dd, J = 8.4, 1.6 Hz, 1H), 7.30 (d, J = 8.7 Hz, 1H), 2.39 (s, 3H) ppm. ^{13}C NMR (DMSO, 400 MHz) δ 170.39, 134.24, 133.26, 129.98, 129.86, 128.33, 126.72, 126.01, 122.91, 117.48, 112.79, 21.45 ppm.

2.7.3. 7-bromonaphtho[2,1-d]thiazol-2(3H)-one

^{1}H NMR (DMSO, 400 MHz) δ 12.25 (s, 1H), 8.23 (d, J = 1.9 Hz, 1H), 7.86 (d, J = 8.7 Hz, 1H), 7.67 (dd, J = 8.8, 2.0 Hz, 1H), 7.58 (d, J = 8.8 Hz, 1H), 7.39 (d, J = 8.7 Hz, 1H) ppm. ^{13}C NMR (DMSO, 400 MHz) δ 170.23, 134.46, 131.29, 130.85, 130.74, 126.69, 126.30, 125.24, 117.81, 117.76, 113.91 ppm.

2.7.4. 7-methoxynaphtho[2,1-d]thiazol-2(3H)-one

^{1}H NMR (DMSO, 400 MHz) δ 12.04 (s, 1H), 7.79 (d, J = 8.6 Hz, 1H), 7.60 (d, J = 9.0 Hz, 1H), 7.39 (d, J = 2.5 Hz, 1H), 7.34 (d, J = 8.7 Hz, 1H), 7.25 (dd, J = 9.0, 2.6 Hz, 1H), 3.89 (s, 3H) ppm. ^{13}C NMR (DMSO, 400 MHz) δ 170.30, 156.69, 132.18, 131.00, 126.25, 124.51, 123.01, 120.27, 117.91, 113.15, 108.09, 55.71 ppm.

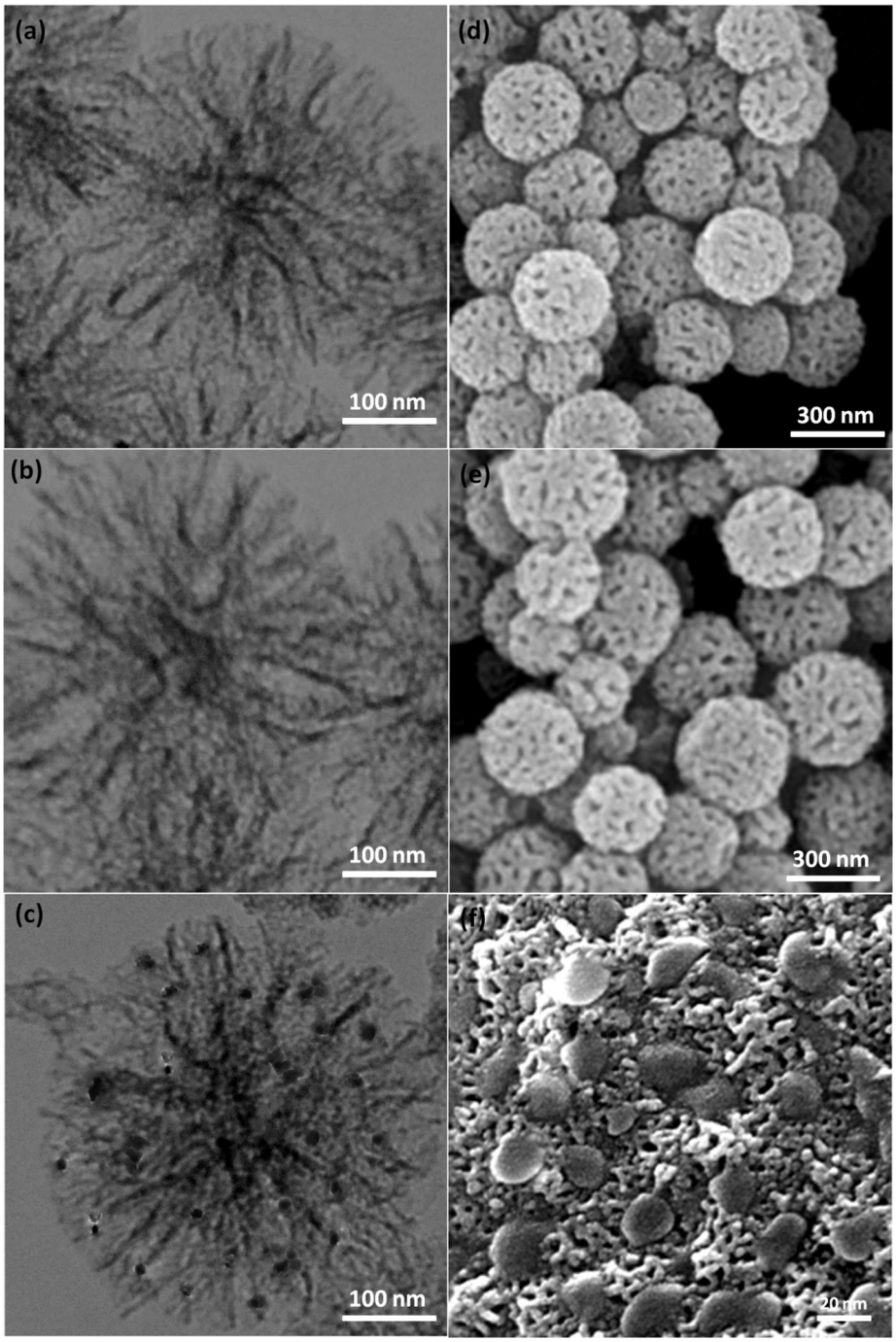

Fig. 1. TEM schemas of DFNS (a), Cellulose/DFNS (b), Au@Cellulose/DFNS (c), and SEM schemas of DFNS (d), Cellulose/DFNS (e), Au@Cellulose/DFNS (f).

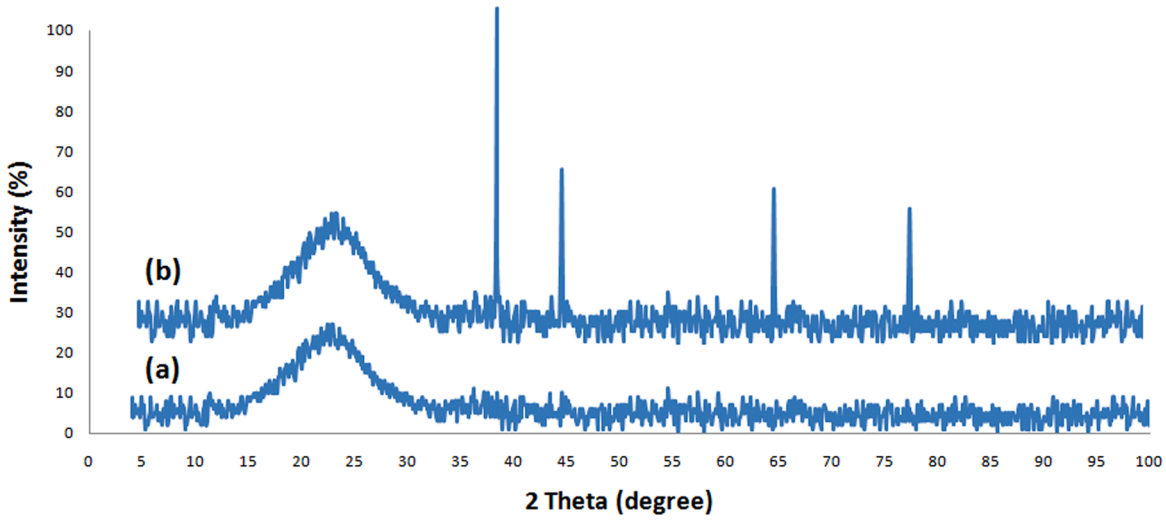

Fig. 2. XRD analysis of (a) DFNS, and (b) Au@Cellulose/DFNS.

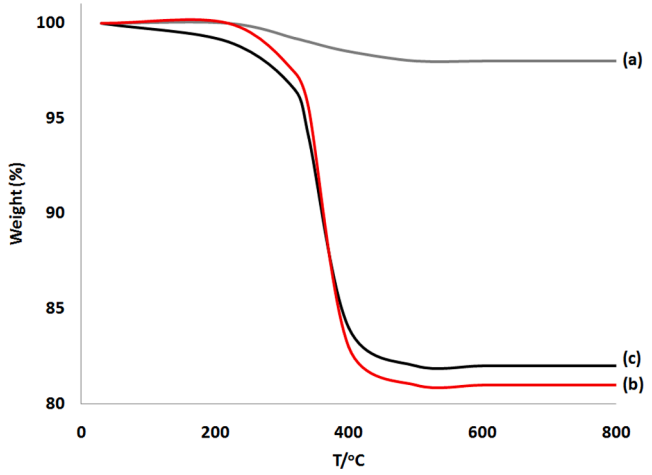

Fig. 3. TGA diagram of (a) DFNS, (b) Cellulose/DFNS, and (c) Au@Cellulose/DFNS NPs.

3. Results and discussion

The catalyst was generated following the model explained in Scheme 2. DFNS was functionalized organically by the condensation reaction of 3-CPTES and hydroxyl groups on the exterior layer of DFNS, followed by the alternative reaction of chloro groups with azide ions to generate N_3/DFNS. The produced N_3/DFNS was then reacted with pre-synthesized alkyne-functionalized cellulose to obtain Cellulose/DFNS through click reaction. Eventually, treatment of Cellulose/DFNS with $HAuCl_4{\cdot}3H_2O$ in absolute ethanol prepared the intended catalyst (Au@Cellulose/DFNS).

The anatomies and morphologies of the Au@Cellulose/DFNS, Cellulose/DFNS, and DFNS NPs were identified employing TEM and SEM. The TEM photo of DFNS (Fig. 1a) specimens showed the wavy radial anatomies of unvarying spheres (300 nm in diameter) and their excellent textures. The thicknesses of wrinkled fibers was about 9 nm. The fibers were organized in 3D dimensions from the center after growth. In addition, open pores were constructed conically employing radial anatomies. The SEM photo depicts the solid fiber essence of the whole sphere (Fig. 1d). Moreover, advanced access to active outer layers and massive displacement of the reactants via the open passage of the hierarchical fiber anatomies was made easy. The SEM and TEM photos of Cellulose/DFNS showed that the morphology of DFNS did not altered after amendment (Fig. 1b and e). Fig. 1c and f depict that TEM and SEM pictures of the gold nanoparticles. It was observed that the as-generated metal nanoparticles were spherical and free of remarkable aggregation. The gold diameter nanoparticles was 15–25 nm. Here, gold nanoparticles were fixed to the fibers of DFNS.

Fig. 2 depicts the XRD pattern of Au@Cellulose/DFNS and DFNS. The wide apex in the range of 20–30° is belonged to amorphous silica as compared to the XRD pattern of DFNS (Fig. 2a). Moreover, Fig. 2b depicts the peaks of $2\theta = 38.1°$, 44.3°, 64.5°, and 77.7° that mirrorthe participation of Au NPs in the anatomy of Au@Cellulose/DFNS catalyst (JCPDS 04-0784). This proves the development of Au particles on the outer layer of Cellulose/DFNS. The broad apex of 20–30° is related to amorphous silica. XRD analysis might be indexed for the cubic phase of Au nanoparticles. Fig. 2b illustrates the participation of Au NPs [sharp peaks of (1 1 1), (2 0 0), (2 2 0), (3 1 1), and (2 2 2)].

Thermogravimetric analysis was performed at various temperatures (from ambient temperature to 700 °C) to affirm the temperature consistency of DFNS, Cellulose/DFNS, and Au@Cellulose/DFNS nanoparticles (see Fig. 3). The weight drop at 180 °C was owing to the elimination of both physisorbed and chemisorbed solvents on the outer layer of the silica material. Organic weight losses (in range of 200–410 °C) of Au@Cellulose/DFNS and Cellulose/DFNS NPs were 18.3% and 17.9%, respectively. The findings affirmed the organic anatomies supported on the DFNS outer layer.

XPS analysis was employed for examining the chemical parts on the Au@Cellulose/DFNS NPs level (Fig. 4). Peaks of Si, C, O, N, and Au and the participation of N 1s additional confirmed that DFNS were functionalized by deploying the Cellulose. Moreover, the participation of nanoparticles of Au was determined deploying a sharp peak proved the presence of gold in the catalyst.

The reaction was examined deploying aniline as the standard substrate with S_8 as the sulfur source under 2 MPa of CO_2 (Table 1). The intended outcome was acquired with 96% efficiency with *t*BuOK as base and CH_3CN as solvent at 80 °C for 8 h (Table 1, entry 16). A variety of bases, such as CsF, Na_2CO_3, Et_3N, NaOAc, KOH, Cs_2CO_3, K_2CO_3, and K_3PO_4, were examined for yields lower than *t*BuOK (Table 1, rows 16–24). The screening of the quantity of *t*BuOK depicted that 4.0 was the premier option (Table 1, entries 25 and 26). Poor results of other solvents, such as THF, DMSO, $CHCl_3$, EtOAc, CH_3CN, and CH_2Cl_2 (Table 1, rows 1–16) highlighted the unique role of CH_3CN in this reaction. The progression of the reaction was controlled by GC for the shortest time in the participation of 10 mg of Au@Cellulose/DFNS. In optimal circumstances, the supreme synthesis efficiency of thiazolidin-2-one could be acquired in 8.0 h (Table 1, entry 27).

The effect of temperature on the reaction is shown in Fig. 5. As

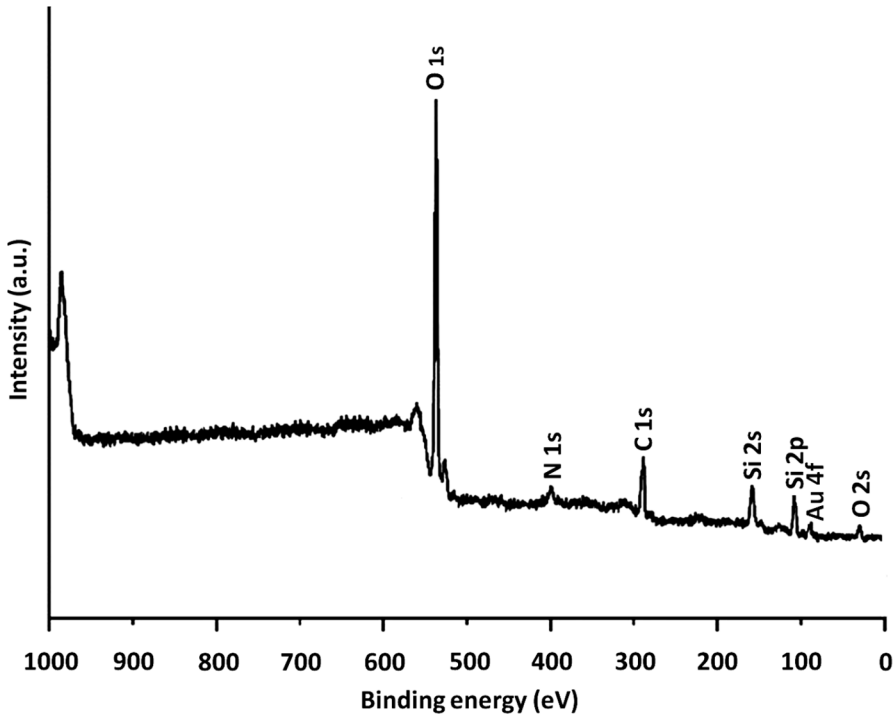

Fig. 4. XPS spectra of Au@Cellulose/DFNS NPs.

Table 1
Synthesis of thiazolidin-2-oneby Au@Cellulose/DFNS NPs with a variety of solvents, bases, and times.[a]

Entry	Solvent	Base	Base (eq.)	Time (h)	Yield (%)[b]
1	solvent-free	*t*BuOK	5	10.0	–
2	EtOH	*t*BuOK	5	10.0	–
3	MeOH	*t*BuOK	5	10.0	–
4	*i*-PrOH	*t*BuOK	5	10.0	–
5	Toluene	*t*BuOK	5	10.0	–
6	*n*-Hexane	*t*BuOK	5	10.0	–
7	Dioxane	*t*BuOK	5	10.0	–
8	CH_2Cl_2	*t*BuOK	5	10.0	51
9	$CHCl_3$	*t*BuOK	5	10.0	49
10	EtOAc	*t*BuOK	5	10.0	60
11	DMSO	*t*BuOK	5	10.0	47
12	H_2O	*t*BuOK	5	10.0	–
13	THF	*t*BuOK	5	10.0	56
14	Anisole	*t*BuOK	5	10.0	74
15	DMF	*t*BuOK	5	10.0	93
16	CH_3CN	*t*BuOK	5	10.0	96
17	CH_3CN	–	5	10.0	–
18	CH_3CN	CsF	5	10.0	33
19	CH_3CN	Na_2CO_3	5	10.0	52
20	CH_3CN	Et_3N	5	10.0	8
21	CH_3CN	NaOAc	5	10.0	17
22	CH_3CN	KOH	5	10.0	31
23	CH_3CN	Cs_2CO_3	5	10.0	32
24	CH_3CN	K_2CO_3	5	10.0	44
25	CH_3CN	*t*BuOK	4	10.0	96
26	CH_3CN	*t*BuOK	3	10.0	87
27	CH_3CN	*t*BuOK	4	8.0	96
28	CH_3CN	*t*BuOK	4	7.0	90

[a] Reaction circumstances: aniline (1.0 mmol), S_8 (1.0 mmol), Au@Cellulose/DFNS (10 mg), solvent (10 mL), with CO_2 (2 MPa) and warmed under reflux.
[b] Isolated efficiencies.

observed, thiazolidin-2-one production enhanced to around 96% at the temperature of 70 °C under 2.0 MPa CO_2 pressure after 8.0 h. In addition, dropping reaction temperature did not lead to better results, which may be due to the inadequate carbonylation and sulfuration with unreactive CO_2 and S_8. Thus, for the parallel reactions of aniline, CO_2 and S_8, the optimum temperature is around 70 °C.

As Fig. 6 depicts, the efficiency was not high in the absence of catalyst. Deploying 2–8 mg of Au@Cellulose/DFNS led to superb yields of synthesis of thiazolidin-2-one. The greatest outcome was acquired in the participation of 8 mg of Au@Cellulose/DFNS. Enhancing the quantity of catalyst did not improved the results, and no product was manufactured in the absence of the catalyst. The effects of CO_2 pressure in the participation of aniline, S_8, and Au@Cellulose/DFNS for 8 h are pictured in Fig. 7. Catalyst mixture reached a yield of 96% at a pressure of 1.5 MPa. In all experiments, no apparent by-products were acquired by GC and the efficiency of thiazolidin-2-one was 96%.

Under best reaction circumstances, the substrate realm and triple-component reaction were investigated (Table 2). It was discovered that a variety of naphthalen-2-amines experience this alteration to manufacture the intended outcomes with supreme efficiency. Particularly, a successful gram-scale reaction of 2-naphthylamine, CO_2, and S_8 resulted in a yield of 91% (Scheme 3). A variety of substituents, including electron-withdrawing groups (EWGs), electron-neutral groups, and electron-donating groups (EDGs) did not influence the reaction. Different functional groups were well tolerated.

For a deeper evaluation of the catalyst's efficiency, a series of control experiments were conducted and the results are depicted in Table 3. The reaction performed with DFNS showed that no amount of the thiazolidin-2-one was formed after 8 h (Table 3, row 1). Moreover, no reaction was perceived when Cellulose/DFNS was employed as catalyst (Table 3, row 2). Cellulose was not able to show good catalytic activity under standard reactions. The results were compared with many other similar catalysts. Due to these unfavorable findings, we continued research to increase the yield by releasing Au (Table 3, Part 3). The outcomes demonstrated that the synthesis of thiazolidin-2-one is primarily catalyzed using Au complexes in the Cellulose/DFNS nanostructure. Nanoparticles improved catalyst activity owing to the

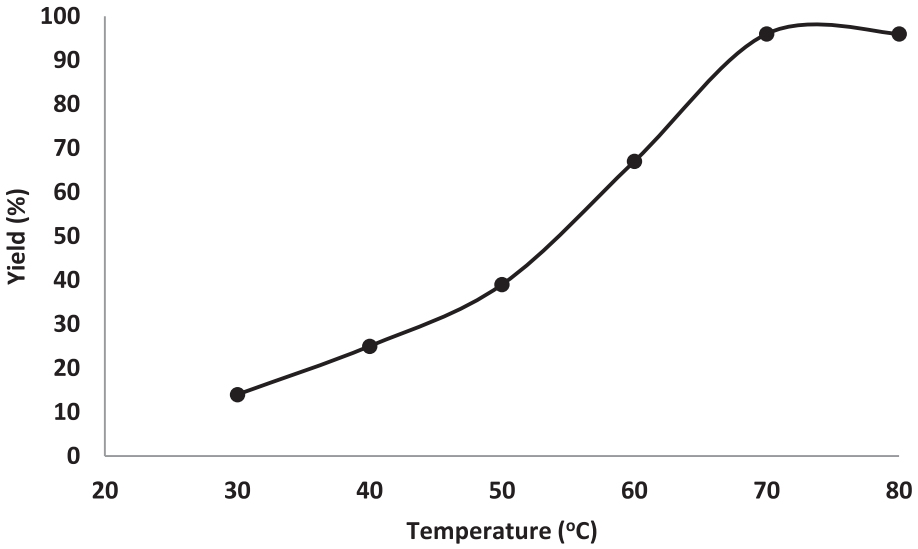

Fig. 5. Effect of temperature on yield of thiazolidin-2-one.

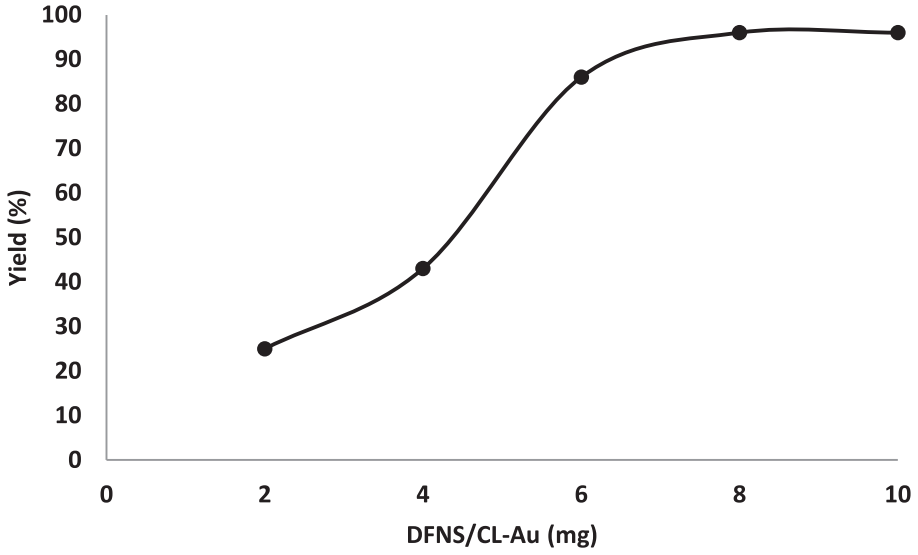

Fig. 6. Effects of the quantity of Au@Cellulose/DFNS NPs on the synthesis of thiazolidin-2-one.

enhancement of outer layer; therefore, they remarkably enhance the susceptibility between the reactants and the catalyst and function as a homogeneous catalyst (Table 3, rows 3 and 4).

The leaching of gold NPs was examined by inductively coupled plasma mass spectrometry (ICP-MS) following 10 runs. Loading quantity of gold NPs was discovered to be 2.2 wt%, indicating the slight leaching of gold NPs. These outcomes affirmed the excellent reusability of gold nanocatalyst (Table 4). Moreover, the loading quantity of gold NPs in Au/DFNS NPs was identified by ICP-MS. The quantity of gold NPs in Au@Cellulose/DFNS was approximately equal to Au/DFNS. The amount of gold NPs in Au@Cellulose/DFNS was about double the Au/DFNS NPs. This outstanding capability of the Au@Cellulose/DFNS mesostructure may be due to the presence of Cellulose units that efficiently block the accumulation of Au and the recovery of gold during the reaction process (Table 4).

In sustainable chemistry, the catalyst reuse mode is a significant charactristic. Hence, the reuse of the Au@Cellulose/DFNS NPs was examined in consonance with the ideal circumstance of thiazolidin-2-one production. Au@Cellulose/DFNS NPs were easily detached after a few seconds. The solvent was capable to be utilized quickly after rinsing. As Fig. 8 depicts, the catalyst was recycled for ten continous runs. The 92% efficiency of the product showed merely a 4% drop.

Additionally, the heterogeneity of the catalyst was detaildly studied. Initially, hot filtration test for the production of thiazolidin-2-one under best circumstances showed the removal of the catalyst at a yield of 48% after 4.0 h. After removal of the heterogeneous catalyst, it was found that the free catalyst residues were relatively active, and the conversion of 50% was achieved after 8.0 h of synthesis of thiazolidin-2-one. This depicted the heterogeneity of catalyst during the reaction, with partial leaching. Eventually, a Mercury-poisoning test was performed to confirm the heterogeneous nature of the catalyst. Mercury (0) significantly attenuates the metal catalyst on the active outer layer and calms its activity, confirming the heterogeneity of catalyst. This test was accomplished on the mentioned reaction model at optimal situations. After 4.0 h, about 300 M mercury was released to the blend and stirred. After 8.0 h, no alteration was perceived in the poisoned catalyst. Fig. 9 depicts the kinetics of the reaction at the attendance of Hg (0). Negative experimental outcomes illustrated that the Au@Cellulose/DFNS was heterogeneous and no significant gold leaching took place during the production of thiazolidin-2-one.

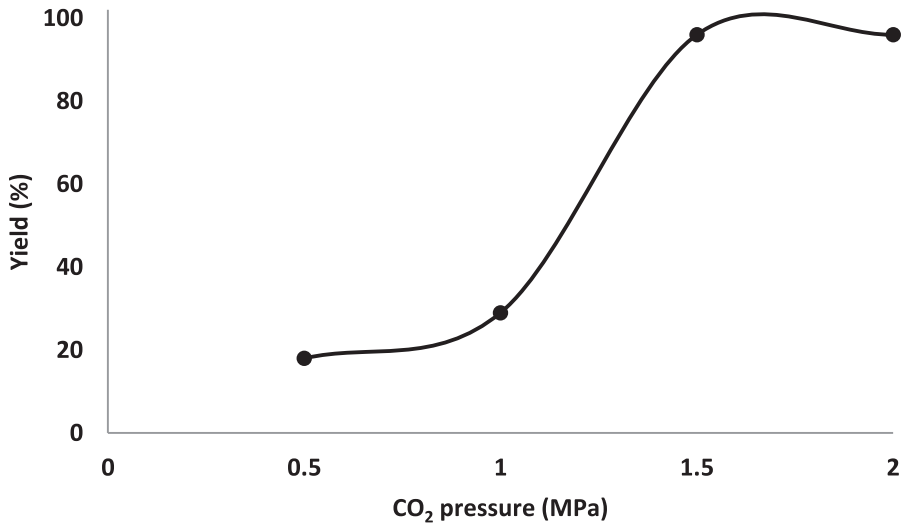

Fig. 7. The impact of CO_2 pressure on the synthesis of thiazolidin-2-one.

Table 2
Substrate scope of naphthalen-2-amines.

Entry	naphthalen-2-amines	Products	Yield (%)
1	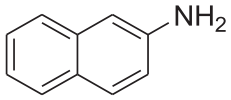	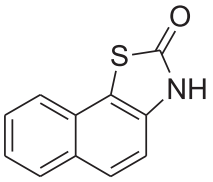	91
2	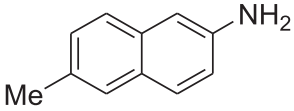	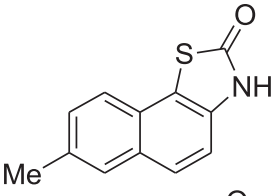	89
3	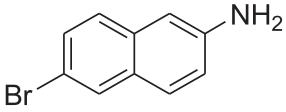	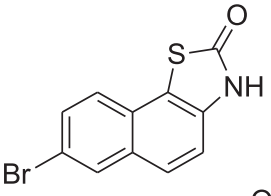	80
4	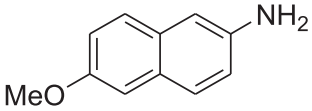	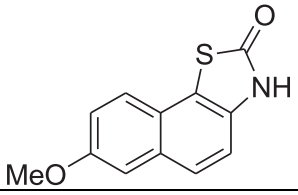	85

[a]Reaction conditions: naphthalen-2-amines (0.5 mmol), S_8 (2.0 mmol), *t*BuOK (4.0 eq.), CO_2 (1.5 MPa), CH_3CN (5 mL), 8 h, 70 °C.
[b]Isolated yields.

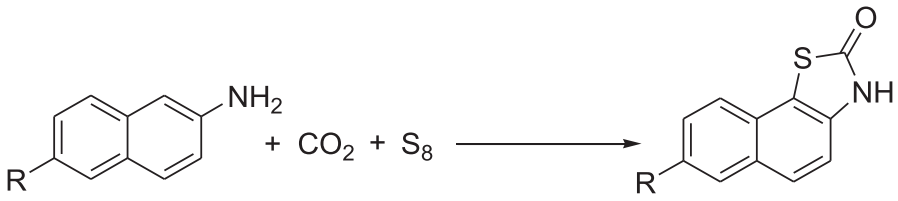

Scheme 3. Production of thiazolidin-2-ones from naphthalen-2-amines, elemental sulfur and CO_2.

Table 3
Effect of various catalysts for the production of thiazolidin-2-one.[a]

Entry	Catalyst	Yield (%)[b]
1	DFNS	–
2	Cellulose/DFNS	–
3	Au@Cellulose/DFNS	96
4	Au@Cellulose	97

[a] Reaction conditions: aniline (1.0 mmol), S_8 (1.0 mmol), *t*BuOK (4.0 eq.), CO_2 (1.5 MPa), CH_3CN (5 mL), 8 h, 70 °C.
[b] Isolated yield.

Table 4
The loading quantity of Au NPs.

Entry	Catalyst	wt%
1	Au/DFNS	2.5
2	Au@Cellulose/DFNS	2.3
3	Au/DFNS after ten reuses	1.1
4	Au@Cellulose/DFNS after ten reuses	2.2

To better comprehend the main reason for the remarkable contrast in recyclability, XPS was utilized to specify the fresh and reused Au@Cellulose/DFNS NPs. The XPS spectra are depicted in Fig. 10. For the fresh Au@Cellulose/DFNS, the Au $4f_{5/2}$ and Au $4f_{7/2}$ binding energies were specified to be 89.4 and 85.7 eV, respectively. Following ten reuses, the 89.4 eV ($4f_{5/2}$) and 85.7 eV ($4f_{7/2}$) binding energies did not altered and corresponded to Au NPs binding energy.

4. Conclusions

Deploying an uncomplicated and sustainable technique free of any reducing medium, Au nanoparticles were supported on DFNS functionalized by cellulose to produce a new separable Au catalyst. We have done the three-component reaction to produce valuable thiazolidin-2-ones from arylamines, S_8, and CO_2 via C(sp^2)–H bond functionalization. The outer layer analysis studies of BET, FTIR, TEM, XPS, SEM, TGA, ICP-MS and EDX showed the functionalization of cellulose and Au in the mesopores silica surface. This technique presents easy accessibility of raw materials, wide substrate range, and good tolerance of functional group, which allows access to a variety of functionalized thiazolidin-2-one derivatives. The preliminary mechanistic studies indicate that isocyanate might be the key intermediate. This rational design in the case of single-site catalysts having full utilization of each Au@Cellulose active site and appropriate recyclability and lower catalyst leaching can

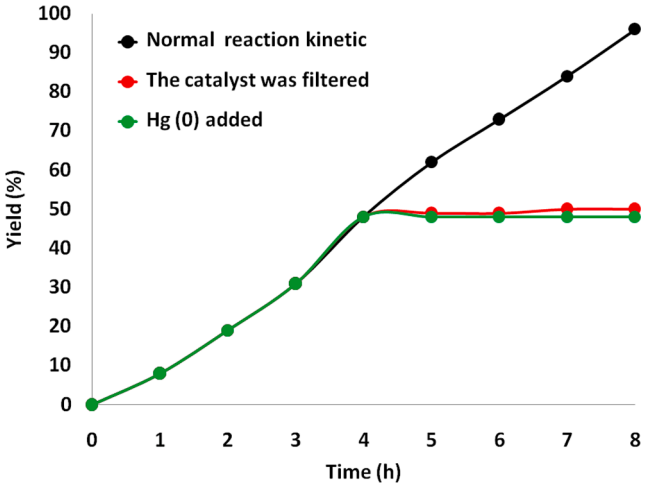

Fig. 9. Leaching test for the catalyst of synthesis of thiazolidin-2-one.

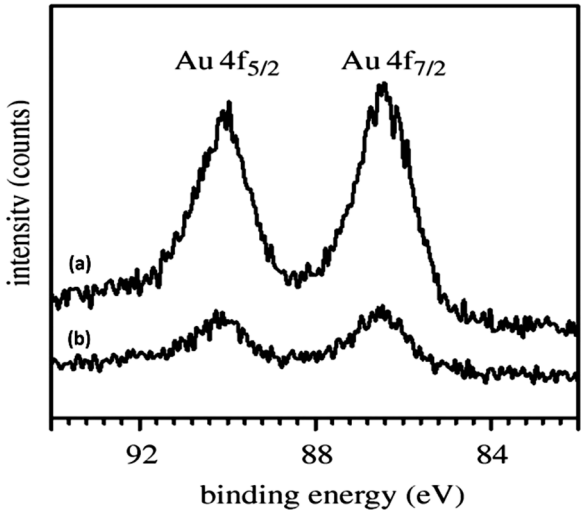

Fig. 10. XPS spectra of the fresh Au@Cellulose/DFNS NPs (a), and Au@Cellulose/DFNS NPs after ten reuses (b).

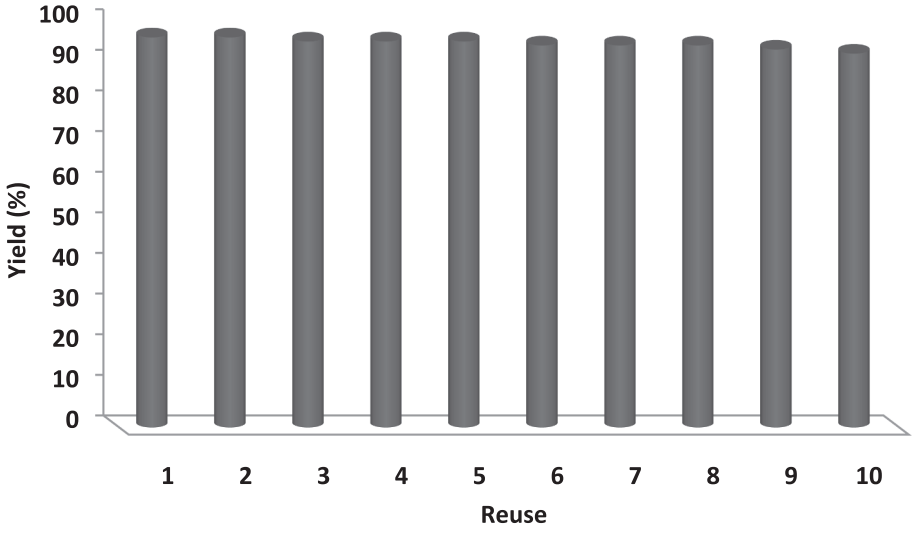

Fig. 8. Recyclability of the catalyst.

occur together with the concepts of green chemistry. The Au@Cellulose/DFNS compared with Au/DFNS for assessing the exact influence of the attendance of Cellulose in the catalyst. The motionless nano gold amount existing in Au@Cellulose/DFNS is around twice Au/DFNS after ten reuses. Form comparing these data, the Cellulose efficiency is proved. Accordingly, by following the method proposed in this study, other NPs with high reusability and efficiency can be developed.

Declaration of Competing Interest

The authors declare that they have no known competing financial interests or personal relationships that could have appeared to influence the work reported in this paper.

Acknowledgement

This work was supported by the Foundation of Chongqing Science and Technology Commission (Chongqing Basic Science and Frontier Technology Research Project: cstc2017jcyjax0429).

References

[1] L. Ackermann, Angew. Chem., Int. Ed. 50 (2011) 3842–3844.
[2] S.M. Saadati, S.M. Sadeghzadeh, Catal. Lett. 148 (2018) 1692–1702.
[3] S.M. Sadeghzadeh, RSC Adv. 5 (2015) 17319–17324.
[4] R. Martín, A.W. Kleij, ChemSusChem 4 (2011) 1259–1263.
[5] T. Tsuji, T. Fujihara, Chem. Commun. 48 (2012) 9956–9964.
[6] S.M. Sadeghzadeh, R. Zhiani, S. Emrani, Catal. Lett. 148 (2018) 119–124.
[7] M. He, Y. Sun, B. Han, Angew. Chem., Int. Ed. 52 (2013) 9620–9633.
[8] S.M. Sadeghzadeh, R. Zhiani, M. Moradi, ChemistrySelect 3 (2018) 3516–3522.
[9] Q.-W. Song, Z.-H. Zhou, L.-N. He, Green Chem. 19 (2017) 3707–3728.
[10] Z. Zhang, J.-H. Ye, D.-S. Wu, Y.-Q. Zhou, D.-G. Yu, Chem. Asian. J. 13 (2018) 2292–2306.
[11] S. Wang, C. Xi, Chem. Soc. Rev. 48 (2019) 382–404.
[12] Y. Takeda, S. Okumura, S. Tone, I. Sasaki, S. Minakata, Org. Lett. 14 (2012) 4874–4877.
[13] L. Sun, J.-H. Ye, W.-J. Zhou, X. Zeng, D.-G. Yu, Org. Lett. 20 (2018) 3049–3052.
[14] L. Zhu, J.-H. Ye, M. Duan, X. Qi, D.-G. Yu, R. Bai, Y. La, Org. Chem. Front. 5 (2018) 633–639.
[15] R. Yousefi, T.J. Struble, J.L. Payne, M. Vishe, N.D. Schley, J.N. Johnston, J. Am. Chem. Soc. 141 (2019) 618–625.
[16] Z. Zhang, T. Ju, J.-H. Ye, D.-G. Yu, Synlett 28 (2017) 741.
[17] L. Song, Y.-X. Jiang, Z. Zhang, Y.-Y. Gui, X.-Y. Zhou, D.-G. Yu, Chem. Commun. 56 (2020) 8355–8367.
[18] T. Onkol, D.S. Dogruer, S. Ito, M.F. Sahin, Arch. Pharm. Med. Chem. 333 (2000) 337–340.
[19] R.V. Bonnert, R.C. Brown, D. Chapman, D.R. Cheshire, J. Dixon, F. Ince, E. C. Kinchin, A.J. Lyons, A.M. Davis, C. Hallam, J. Med. Chem. 41 (1998) 4915–4917.
[20] S.M. Sadeghzadeh, J. Mol. Liquids 223 (2016) 267–273.
[21] S. Inoue, T. Kato, J. Pestic. Sci. 8 (1983) 333–338.
[22] S. Inoue, T. Uematsu, T. Kato, J. Pestic. Sci. 9 (1984) 689–695.
[23] H. Liu, X. Jiang, Chem. – Asian J. 8 (2013) 2546–2563.
[24] T.B. Nguyen, Adv. Synth. Catal. 359 (2017) 1066–1130.
[25] T.B. Nguyen, Asian J. Org. Chem. 6 (2017) 477.
[26] L.-L. Sun, C.-L. Deng, R.-Y. Tang, X.-G. Zhang, J. Org. Chem. 76 (2011) 7546–7550.
[27] T.B. Nguyen, L. Ermolenko, P. Retailleau, A. Al-Mourabit, Angew. Chem., Int. Ed. 53 (2014) 13808–13812.
[28] Y. Yang, X. Zhang, W. Zeng, H. Huang, Y. Liang, RSC Adv. 4 (2014) 6090–6093.
[29] Y. Liao, Y. Peng, H. Qi, G.-J. Deng, H. Gong, C.-J. Li, Chem. Commun. 51 (2015) 1031–1034.
[30] F. Chen, G. Liao, X. Li, J. Wu, B.-F. Shi, Org. Lett. 16 (2014) 5644–5647.
[31] L. Meng, T. Fujikawa, M. Kuwayama, Y. Segawa, K. Itami, J. Am. Chem. Soc. 138 (2016) 10351–10355.
[32] H. Xie, J. Cai, Z. Wang, H. Huang, G.-J. Deng, Org. Lett. 18 (2016) 2196–2199.
[33] L.P. Liu, G.B. Hammond, Chem. Soc. Rev. 41 (2012) 3129–3139.
[34] A.S.K. Hashmi, L. Schwarz, J.H. Choi, T.M. Frost, Angewandte Chemie Int. Ed. 39 (2000) 2285–2288.
[35] A.S.K. Hashmi, G.J. Hutchings, Angewandte Chemie Int. Ed. 45 (2006) 7896–7936.
[36] W.B. Wang, G.B. Hammond, B. Xu, J. Am. Chem. Soc. 134 (2012) 5697.
[37] L. Guczi, A. Beck, Z. Paszti, Catal. Today 181 (2012) 26–32.
[38] A.S.K. Hashmi, A.M. Schuster, S. Litters, F. Rominger, M. Pernpointner, Chem. A Eur. J. 17 (2011) 5661–5667.
[39] S.E. Baghbamidi, A. Hassankhani, E. Sanchooli, S.M. Sadeghzadeh, Appl. Organometallic Chem. 32 (2018), e4251.
[40] Y. Zhang, C. Zhu, Catal. Commun. 28 (2012) 134–137.
[41] T. Yamamoto, T. Yamada, Y. Nagata, M. Suginome, J. Am. Chem. Soc. 132 (2010) 7899–7901.
[42] X. Zhang, P. Li, Y. Ji, L. Zhang, L. Wang, Synthesis (2011) 2975–2983.
[43] M.S. Sadeghzadeh, RSC Adv. 5 (2015) 68947–68952.